IEEE Access
Multidisciplinary | Rapid Review | Open Access Journal

Received March 21, 2017, accepted April 1, 2017, date of publication April 18, 2017, date of current version May 17, 2017.

Digital Object Identifier 10.1109/ACCESS.2017.2693687

Composite Active Front Steering Controller Design for Vehicle System

XIAOYAN DIAO[1], YANG JIN[1], LI MA[1], SHIHONG DING[1], AND HAOBIN JIANG[2]
[1]School of Electrical and Information Engineering, Jiangsu University, Zhenjiang 212013, China
[2]School of Automotive and Traffic Engineering, Zhenjiang 212013, China

Corresponding author: Li Ma (mali@mail.ujs.edu.cn)

This work was supported in part by the National Natural Science Foundation of China under Grant 61573170 and Grant 51375210, in part by the China Postdoctoral Science Foundation under Grant 2015M571687 and Grant 2016T90427, in part by the Priority Academic Program Development of Jiangsu Higher Education Institutions, and in part by the Zhejiang Open Foundation of the Most Important Subjects.

ABSTRACT The active front steering (AFS) technique is one of the effective methods to handle the stability of a vehicle. In this paper, some AFS control schemes have been proposed. First, a two degree of freedom mathematical model for the vehicle dynamics has been introduced in order to calculate the desired yaw rate. On this basis, the actual sideslip angle is further identified and estimated by constructing a sliding-mode observer. Then, two kinds of baseline AFS controllers are proposed by using PID and terminal sliding mode techniques, such that the actual yaw rate will approach its reference value as closely as possible. To further improve the performance of the closed-loop AFS control system, taking the uncertainties and external disturbances into account, the composite control schemes are developed by combining the previous designed state-feedback controllers and feedforward compensation term generated by the disturbance observer. The effectiveness of the designed AFS control schemes is verified by using the Carsim Software. It has been verified that the performance under two composite controllers is better than both baseline controllers.

INDEX TERMS AFS, terminal sliding mode, disturbance observer, finite-time control.

I. INTRODUCTION

Vehicle stability control is an active safety system that helps reduce the amount of wheel slip during acceleration and in harsh driving, such that the driver will stay in control of his/her vehicle during a critical manoeuver. The research on improving the stability of a vehicle, which is also called active safety control, has attracted much attention in recent years and a great of progresses in stability control of vehicles have been made, such as [1]–[5]. Generally speaking, the active safety control mainly includes anti-lock braking [1], direct yaw moment control [2], active suspension system [3], [4] and active front steering (AFS) [5]. AFS is one of the frequently-used effective methods for active safety control, because it can modify the steering angle of the driver by providing an additional angle that does not depend on the input of the steering wheel angle, so as to help the driver to avoid getting into critical handling situations. Consequently, the AFS techniques have been extensively studied both from auto industry and academia [6]–[8].

In the early stage, the PI (proportion integration) control technique has been widely employed in the AFS controller design by regarding vehicle dynamics as a linear system. For example, a PI feedback controller was designed in [9] to make sure that the yaw rate error will converge to zero. However, the parameters of the PI controller are not easy to tune. As a matter of fact, it should be noted that the vehicle dynamics are a class of complicated nonlinear systems with lumped disturbance including system uncertainties, parameter perturbations, speed variations and external disturbances, which always affect the control performance of the closed-loop system [10]–[12]. This implies that the performance under linear controller may not be satisfactory, especially under some extreme working conditions. To this end, several nonlinear control methods are introduced for AFS control design problem, such as fuzzy control [13], optimal control [14], H_∞ control [15], nonsmooth control [19] and sliding mode control (SMC) [16], etc. Among them, the SMC method has been considered as one of the effective methods to deal with uncertainties or disturbances.

SMC is a nonlinear control method which alters the dynamics of a system by using a discontinuous control signal and forces the system states to slide along a prescribed

2169-3536 © 2017 IEEE. Translations and content mining are permitted for academic research only.
Personal use is also permitted, but republication/redistribution requires IEEE permission.
See http://www.ieee.org/publications_standards/publications/rights/index.html for more information.

switching manifold. It is known that SMC possess several advantages, such as rapid convergence, good disturbance rejection and easy implementation. In addition, it does not require the considered system having an accurate mathematical model. Consequently, SMC techniques have been widely applied in active safety control design [16]–[18]. In [17], a new robust sliding mode controller is designed for a class of linear systems and then applied to the path tracking problem of 4WS (Four Wheel Steering) vehicles. Later, the SMC theory is applied to the active front and rear wheel steering control problem in [16] such that the yaw rate and the sideslip angle can both track their desired values. Meanwhile, a continuous sliding mode direct yaw-moment controller is designed in [18] to guarantee that the sideslip angle and the yaw rate will approach the ideal ones as closely as possible.

It can be clearly observed from [16]–[18] that the linear sliding surface is always adopted in the traditional SMC. This implies that the sliding variables will slide to the origin asymptotically when they reach the linear sliding surface. In other words, the states will converge to the origin in an infinite time no matter how to tune the parameters in the traditional SMC. Meanwhile, the robust property of the closed loop SMC system may also not be satisfactory when the sign function is replaced by using a saturation function in order to alleviate the chattering. To further improve the convergence and robustness of the closed-loop SMC system, the terminal sliding mode (TSM) has been developed in [20]–[22]. By introducing a nonlinear sliding surface in TSM, the system states can converge to the origin in a finite time along the sliding surface. It has been proved in many applications that by comparing with the conventional linear sliding mode, the TSM control exhibits various superior properties such as faster response, better disturbance rejection and more control accuracy [23], [24]. However, similar to the conventional SMC, the chattering problem always occurs. The conventional way to avoid the chattering problem is the boundary layer method by replacing the sign function in the SMC controller with a saturation function. However, the robustness of the closed-loop system will be partly reduced. Noth that the amplitude of the chattering is mainly determined by the control gains of SMC controller, while the values of the control gains are depended on the bound of the disturbances. If the disturbances can be observed and be partly compensated, then the values of the control gains in sliding mode controller can be chosen to be some smaller ones. In this case, the chattering problem can surely be attenuated.

In this paper, four categories of control schemes are proposed for vehicle AFS system. First of all, since the sideslip angle is usually not easy to be measured by using sensors, the sliding mode (SM) observer is applied to estimate the exact value of the vehicle sideslip angle. Based on this, two baseline controllers are given. The first one is the PI control by regarding the yaw rate error as the deviation. However, the tracking performance is not satisfactory under some large lumped disturbances. The second one is the TSM control scheme. Although it can be proved that under TSM controller the yaw rate error will converge to the origin in a finite time, the control parameters are required to be tuned large enough to restrain the disturbances, which results in a heavy chattering problem. To fix the problems existing in the baseline control methods, two composite control schemes are proposed by combining the aforementioned baseline controllers and the disturbance observer (DOB) technique [25]. A DOB will first be constructed such that the lumped disturbances can be well estimated. And then, the estimated value will be regarded as a feedforward term to compensate the unknown lumped disturbances. Finally, the baseline feedback controllers plus the feedforward compensation composite the composite control schemes. The theoretical results have been verified by a commercial vehicle dynamic software.

II. VEHICLE DYNAMICS AND PROBLEM FORMULATION

In this section, a 2DOF vehicle model (the bicycle model) consisting of lateral and yaw motions is first described, which is used for calculating the reference yaw rate. Then the problem statement is followed.

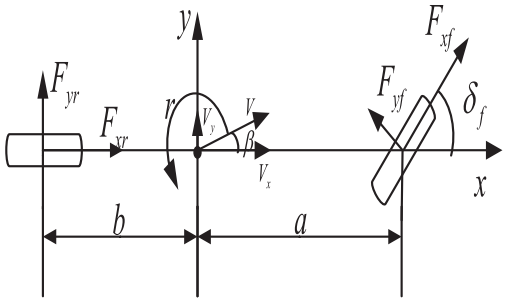

FIGURE 1. 2DOF vehicle model.

A. 2DOF VEHICLE MODEL

In normal 'on road' driving, the vehicle's handling dynamics can be represented by a two degree-of-freedom single track model, known famously as the 'bicycle model' shown in Fig. 1. It is depicted in Fig. 1 that β is the sideslip angle; r is yaw rate; m is the vehicle mass, the distances from the center of gravity to the front and rear axles are given by a and b respectively; δ_f is the front wheel steering angle; I_z is the moment of inertia of the vehicle, V_x and V_y are the longitudinal and lateral velocities at the center of gravity of vehicle. In addition, F_{xf}, F_{yf} and F_{xr}, F_{yr} represent the front and rear tire forces, respectively.

To describe the dynamics of 'bicycle model', the following assumptions have to be made [26]

- Ignore the influence of the steering system;
- Ignore the effect of suspension;
- Ignore the changes of tires characteristic and the effect of the aligning torque caused by the load change;
- Only consists of lateral motion and yaw motion.

On these bases, the vehicle motion equations are described as follows

$$mV_x(\dot{\beta}+r) = -2(C_f+C_r)\beta + \frac{-2(aC_f-bC_r)}{V_x}r + 2C_f\delta_f \quad (1)$$

$$I_z\dot{r} = -2(aC_f-bC_r)\beta + \frac{-2(a^2C_f+b^2C_r)}{V_x}r + 2aC_f\delta_f \quad (2)$$

where C_f and C_r respectively are the front and rear tyre cornering stiffness.

B. PROBLEM FORMULATION

The AFS system realizes front-wheel steering control by superimposing an "active angle" to the steering-wheel input (δ_s) from the driver. Unlike steer-by-wire, the AFS system is distinguished by a permanent mechanical connection between the steering wheel and road wheels, owing to an innovative design of the planetary gear set [27]. The purpose of AFS control is to ensure the stability of the vehicles, in such a way that the actual yaw rate should track its reference value. The reference yaw rate can be calculated by the steering wheel angle, vehicle speed and the other vehicle parameters as follows [28]

$$r_t = \frac{V_x}{(a+b)(1+KV_x^2)}\delta_s \quad (3)$$

where $K = m(bC_r - aC_f)/\left(2C_fC_r(a+b)^2\right)$ is the vehicle insufficient steering coefficient and δ_s is the steering wheel input. Considering the tyre/road condition, the reference yaw rate is limited as follows

$$r_d = \begin{cases} r_t, & |r_t| < \dfrac{0.85\mu g}{V_x} \\ \dfrac{0.85\mu g}{V_x}sign(r_t), & |r_t| \geq \dfrac{0.85\mu g}{V_x} \end{cases} \quad (4)$$

where μ is the road adhesion coefficient and g is the gravitational constant.

On the other hand, the actual sideslip angle of the vehicle is generally difficult to be measured by sensors. The usual method to obtain the information of the sideslip angle is the way of designing a state observer.

The goal of the paper is to design the AFS controller such that the actual yaw rate will track the reference yaw rate (4) *as closely as possible.* The diagram of control design is depicted in Fig. 2.

III. CONTROL SYSTEM DESIGN

A. SIDESLIP ANGLE OBSERVER

Normally, the yaw rate r and the lateral acceleration a_y can be measured directly through sensors. In addition, a_y can be expressed as

$$a_y = V_x(\dot{\beta}+r) = \frac{-2(C_f+C_r)}{m}\beta + \frac{-2(aC_f-bC_r)}{mV_x}r + \frac{2C_f}{m}\delta_f. \quad (5)$$

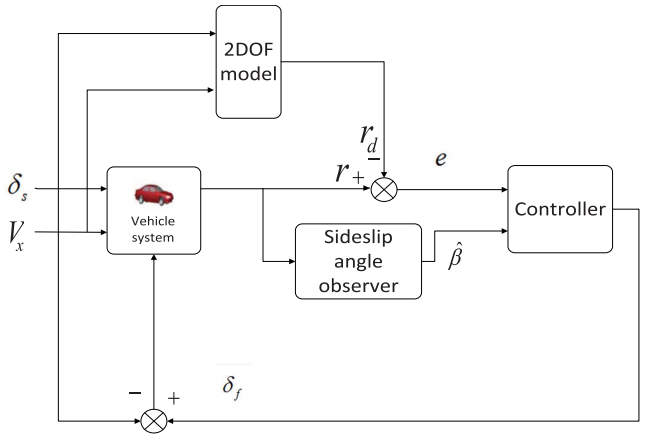

FIGURE 2. Structure of AFS control system.

Introducing the variables $x_1 = r$, $x_2 = \beta$, $X = [r, \beta]^T$, $Y = [y_1, y_2]^T = [r, a_y]^T$, $u = [\delta_f]$. The vehicle model described by Eqs. (1)-(2) and (5) can be rewritten as

$$\begin{cases} \dot{X} = AX + Bu \\ Y = CX + Du \end{cases}$$

$$A = \begin{bmatrix} \dfrac{-2(a^2C_f+b^2C_r)}{I_zV_x} & \dfrac{-2(aC_f-bC_r)}{I_z} \\ \dfrac{-2(aC_f-bC_r)}{mV_x^2} - 1 & \dfrac{-2(C_f+C_r)}{mV_x} \end{bmatrix},$$

$$B = \begin{bmatrix} \dfrac{2aC_f}{I_z} \\ \dfrac{2C_f}{mV_x} \end{bmatrix},$$

$$C = \begin{bmatrix} 1 & 0 \\ V_x(A_{21}+1) & V_xA_{22} \end{bmatrix}, \quad D = \begin{bmatrix} 0 \\ V_xB_2 \end{bmatrix}. \quad (6)$$

The sideslip angle observer can be designed as follows

$$\begin{cases} \dot{\hat{x}}_1 = A_{11}y_1 + A_{12}\hat{x}_2 + B_1u + c_1|y_1-\hat{x}_1|^{\frac{1}{2}}sign(y_1-\hat{x}_1) \\ \dot{\hat{x}}_2 = A_{21}y_1 + A_{22}\hat{x}_2 + B_2u + c_2sign(y_1-\hat{x}_1) \\ \quad + \dfrac{1}{V_x}(a_y-\hat{a}_y) \\ \hat{a}_y = V_x(A_{21}+1)y_1 + V_xA_{22}\hat{x}_2 + V_xB_2\delta_f \end{cases} \quad (7)$$

where the value of a_y can be directly obtained by a sensor, $\hat{x}_1$ and $\hat{x}_2$ are the estimation of r and β respectively, $\hat{a}_y$ is the estimate of a_y, c_1 and c_2 are two positive constants. Then we have the following lemma.

Lemma 1: If the sliding model observer is designed as (7), then the state x_2 will be identical to $\hat{x}_2$ in a finite time.

Proof: Let $\tilde{x}_1 = x_1 - \hat{x}_1, \tilde{x}_2 = x_2 - \hat{x}_2$. Taking the derivative of $\tilde{x}_1$ and $\tilde{x}_2$ yields

$$\begin{cases} \dot{\tilde{x}}_1 = A_{12}\tilde{x}_2 - c_1|\tilde{x}_1|^{\frac{1}{2}}sign(\tilde{x}_1) \\ \dot{\tilde{x}}_2 = F(\tilde{x}_2) - c_2sign(\tilde{x}_1) \end{cases} \quad (8)$$

where $F(\tilde{x}_2) = A_{22}\tilde{x}_2$. The sideslip angle is usually small, so it can be assumed that there is a positive constant $\bar{F}$ such that

$$|F(\tilde{x}_2)| \leq \bar{F}. \quad (9)$$

Then we will prove the finite-time convergence of system (8) under condition (9).

Introducing $E_1 = \frac{\tilde{x}_1}{A_{12}\bar{F}}$ and $E_2 = \frac{\tilde{x}_2}{\bar{F}}$. By (8) and (9), one obtains

$$\begin{cases} \dot{E}_1 = E_2 - \dfrac{c_1}{A_{12}^{1/2}\bar{F}^{1/2}}|E_1|^{\frac{1}{2}}sign(E_1) \\ \dot{E}_2 \in [-1,+1] - \dfrac{c_2}{\bar{F}}sign(E_1) \end{cases} \tag{10}$$

Note that $sign(E_1) = sign(E_2 - \dot{E}_1)$. Thus Eq. (10) can be written as follows

$$\begin{cases} \dot{E}_1 = E_2 - \dfrac{c_1}{A_{12}^{1/2}\bar{F}^{1/2}}|E_1|^{\frac{1}{2}}sign(E_1) \\ \dot{E}_2 \in [-1,+1] - \dfrac{c_2}{\bar{F}}sign(E_2 - \dot{E}_1) \end{cases} \tag{11}$$

The rest of the proof is omitted for brevity since the proof procedure actually does not much differ form that of Theorem 6.4 in [29]. □

B. BASELINE CONTROLLER DESIGN

In this subsection, two baseline controllers will be proposed. First of all, the PI controller will be given. Then, the TSM controller will be further considered in order to improve the disturbance rejection property of the closed loop system.

1) PI CONTROL

It can be observed from the literature that the PID control technique has been widely used in AFS control design. Note that the actual yaw rate should close to its reference value. Hence, the deviation variable is usually chosen as

$$e_1(t) = r - r_d \tag{12}$$

Then the controller (i.e., the steering angle δ_f) can be designed as

$$\delta_f = K_p e_1(t) + K_i \int e_1(t)dt \tag{13}$$

where K_p and K_i are proportion coefficient and integration coefficient, respectively. By tuning the parameters K_p and K_i, the deviation $e(t)$ will converge to zero, which implies the actual yaw rate will approach the reference value.

On the other hand, the PID control is usually based on the linear model by linearization technique, while the vehicle dynamics is in essence a nonlinear system. This implies that the performance of the closed loop system based on PI controller may be undesirable under some extreme conditions. To improve the control accuracy of PI controller, a terminal sliding mode control scheme will be proposed in the following subsection.

2) TSM CONTROL

We choose the terminal sliding surface as

$$s = e_1 + c \cdot \int_0^t sign(e_1)|e_1|^{\alpha}dt,\ 0 < \alpha < 1,\ c > 0 \tag{14}$$

Taking the derivative of (14) along system (2) yields

$$\dot{s} = A_{11}r + A_{12}\beta + B_1\delta_f + c \cdot sign(e_1)|e_1|^{\alpha} + D_1(t) \tag{15}$$

where $D_1(t) = d(t) - \dot{r}_d$ and $d(t)$ is the bounded lumped disturbance including system uncertainties and external disturbance in the yaw rate dynamics. It is also assumed that $\dot{D}_1(t)$ is bounded. Meanwhile, we let $D_2(t) = D_1(t) + A_{12}(\beta - \hat{\beta})$. Note that $d(t)$ and $\dot{r}_d$ are bounded. And from Lemma 1, it can be obtained that β will track $\hat{\beta}$ in a finite time. So, we can find a constant γ_{D_2} such that

$$|D_2(t)| \le \gamma_{D_2}$$

Then we have the following result.

Theorem 1: If the TSM controller is designed as

$$\begin{aligned} \delta_f = \frac{1}{B_1}(&-A_{11}r - A_{12}\hat{\beta} - c \cdot sign(r - r_d)|r - r_d|^{\alpha} \\ &- K_1 \cdot sign(s) - K_2 s) \end{aligned} \tag{16}$$

where $k_1 > \gamma_{D_2}, k_2 > 0$, then the yaw rate r will converge to its reference signal r_d in a finite time.

Proof: With $e_1 = r - r_d$ in mind, substituting (16) into (15) yields

$$\dot{s} = -K_1 \cdot sign(s) - K_2 s + D_2(t) \tag{17}$$

Consider the following Lyapunov function as

$$V_1(s) = \frac{1}{2}s^2.$$

Taking the derivative of $V(s)$ along system (17) yields

$$\begin{aligned} \dot{V}_1 &= s\dot{s} \\ &= -k_1 \cdot sign(s) \cdot s - k_2 s^2 + D_2(t)s \\ &\le -k_1|s| - k_2 s^2 + |D_2(t)||s| \\ &\le -(k_1 - \gamma_{D_2})|s| - k_2 s^2 \\ &\le -(k_1 - \gamma_{D_2})|s| \end{aligned}$$

Note that $k_1 > \gamma_{D_2}$. We can verify that

$$\dot{V}_1 + c_\gamma V_1^{1/2} \le 0,\quad c_\gamma = \sqrt{2}(k_1 - \gamma_{D_2}).$$

According to the finite-time Lyapunov stability theory proposed in [30], the TSM variable s will converge to the origin in a finite time. This implies that there exists a finite time instant T such that $s(T) = 0$ and $s(t) \equiv 0, \forall t > T$. When $s \equiv 0$, we have $s \equiv e_1 + c \cdot \int_0^t sign(e_1)|e_1|^{\alpha}dt \equiv 0$. It implies $\dot{e}_1 + csign(e_1)|e_1|^{\alpha} \equiv 0$. By a simple calculation, we can obtain the yaw rate error will converge to zero in a finite time $T + \frac{|e_1(0)|^{1-\alpha}}{(1-\alpha)c}$. □

Remark 1: It can be clearly seen from Theorem 1 that the gain k_1 of controller (16) should be chosen to guarantee the condition $k_1 > \gamma_{D_2}$. However, the upper bound of the disturbance γ_{D_2} is usually difficult to be determined or estimated much conservative. It means that γ_{D_2} may be very large. In this case, the sliding gain k_1 is required to be tuned largely in order to suppress the lumped disturbances. As a result, the chattering problem will be very heavy.

Remark 2: For TSM controller (16), we can first choose a small K_1, a proper K_2 and $\alpha = 1$ such that the sliding variable will not diverge. Then, We can tune the parameter K_1 from small to large to guarantee that the sliding variable will converge to zero. Finally, we can further tune the fractional power α until the best convergence and robustness performance of the closed-loop system can be obtained.

C. COMPOSITE CONTROLLER DESIGN

We should note that if the lumped disturbance is large, the control performance under PI controller (13) will not be satisfactory. Although the control performance under TSM controller (16) is acceptable, the chattering will be heavy. In the following, by combining the baseline controllers and DOB technique, the composite controllers will be given to further improve the performance of the closed loop system.

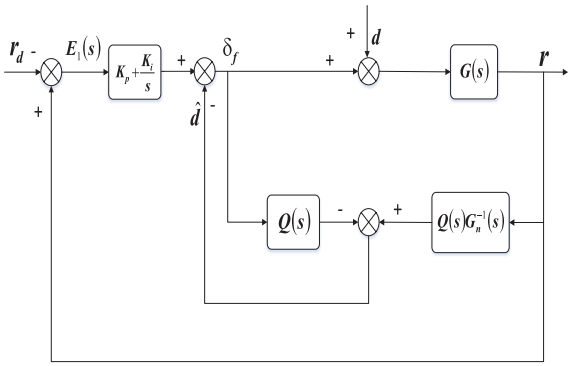

FIGURE 3. The block diagram of DOB-based PI control.

1) DOB-BASED PI CONTROL

To get rid of the influence of the lumped disturbance, one of the effective methods is the DOB-based control. The DOB is used to estimate the unknown lumped disturbance, and then the estimated value can be utilized to compensate it [31]. The block diagram of DOB-based PI control scheme is depicted in Fig. 3 Here, δ_f is the control input, r is the controlled output, d is the lumped disturbance in the yaw rate dynamics, $G(s)$ is the mathematical model of plant, $G_n(s)$ is the nominal model of plant and $Q(s)$ is the filter of DOB, respectively. In addition, $\hat{d}$ is the estimated value of the lumped disturbance. In the absence of the lumped disturbance, by using Laplace transforms and noting the fact that $u = \delta_f$, system (6) can also be written as

$$sX(s) = AX(s) + B\delta_f(s) \tag{18}$$

$$Y(s) = CX(s) + D\delta_f(s). \tag{19}$$

From (18), one has

$$X(s) = (sI - A)^{-1}B\delta_f(s) \tag{20}$$

By (19) and (20), it follows

$$Y(s) = C(sI - A)^{-1}B\delta_f(s) + D\delta_f(s) \tag{21}$$

Hence, the transfer function of the system is

$$G(s) = \frac{Y(s)}{\delta_f(s)} = C(sI - A)^{-1}B + D \tag{22}$$

On the other hand, by taking $G_n(s) = G(s)$, it follows from Fig. 3 that

$$\begin{aligned}\hat{d}(s) &= Q(s)G_n^{-1}(s)r(s) - Q(s)\delta_f(s)\\ &= Q(s)G_n^{-1}(s)G(s)(\delta_f(s) + d(s)) - Q(s)\delta_f(s)\\ &= Q(s)d(s)\end{aligned} \tag{23}$$

It is derived from (23) that

$$E_d(s) = \hat{d}(s) - d(s) = [Q(s) - 1]d(s) \tag{24}$$

The estimation error $E_d(s)$ will tend to zero as time goes to infinity if the filter $Q(s)$ is selected as a low-pass form, that is, $\lim_{s\to\infty} Q(s) = 1$.

Actually, $Q(s)$ can be designed in such a way that [31]:

- The relative degree of $Q(s)$ should be no less than that of the nominal model $G_n(s)$ and $Q(s)G_n^{-1}(s)$ should be proper.
- In the domain of low-frequency, $Q(s)$ should close to 1, guaranteeing that the estimate of lumped disturbance approximately equals to the lumped disturbance.

By following the above rules, the low-pass filter can be chosen as the following form

$$Q(s) = \frac{1}{\lambda s + 1} \tag{25}$$

where λ is the filter parameter. The parameter λ in filter $Q(s)$ should be chosen to be a small one such that it will possess low-pass property. According to our experiences, $\lambda = 0.01$ or 0.02 will be enough. Then the DOB-based controller can be designed as

$$\delta_f = K_p e_1(t) + K_i \int e_1(t)dt - \hat{d}(t) \tag{26}$$

2) DOB-BASED TSM CONTROL

By letting $x = s$, system (15) can be rewritten as

$$\dot{x} = F(x) + G_1(x)\delta_f + G_2(x)D_2(t) \tag{27}$$

where $F(x) = A_{11}r + A_{12}\hat{\beta} + c \cdot sign(r - r_d)|r - r_d|^{\alpha}$, $G_1(x) = B_1$ and $G_2(x) = 1$. Note that the sideslip angle β is usually change slowly and $\dot{D}_1$ is also bounded. Hence, it is reasonable to assume that the lumped disturbance $D_2(t) = A_{12}(\beta - \hat{\beta}) + D_1(t)$ satisfies $|\dot{D}_2(t)| \le \gamma_{\dot{D}_2}$ with $\gamma_{\dot{D}_2}$ being a positive constant. This property holds at least locally.

Based on the nonlinear disturbance observer (NDOB) theory, the NDOB can be designed as

$$\begin{cases}\dot{P} = -LG_2P - L[G_2Lx + F(x) + G_1(x)\delta_f],\\ \hat{D}_2 = P + Lx\end{cases} \tag{28}$$

where $\hat{D}_2$ is the estimation of the lumped disturbance, P is the internal state of NDOB and L is the observer gain satisfying $L > \gamma_{\dot{D}_2}$.

Let the estimation error be $e_2(t) = D_2(t) - \hat{D}_2(t)$. Taking the derivative of $e_2(x)$ along systems (27) and (28) has

$$\begin{aligned}\dot{e}_2 &= \dot{D}_2 - \dot{\hat{D}}_2 \\ &= \dot{D}_2 - \left[-LG_2P - L^2G_2x + LG_2D_2\right] \\ &= \dot{D}_2 - LG_2e_2 \end{aligned} \tag{29}$$

Select a Lyapunov function as

$$V_2(e_2) = \frac{1}{2}e_2^2.$$

Taking the derivative of $V_2(e_2)$ along equation (29) yields

$$\begin{aligned}\dot{V}_2 &= e_2\dot{e}_2 \\ &= e_2(\dot{D}_2 - LG_2e_2) \\ &\leq |e_2|\gamma_{\dot{D}_2} - LG_2e_2^2 \end{aligned} \tag{30}$$

Define a region as $Q_1 = \left\{e_2 : |e_2| \leq \frac{\gamma_{\dot{D}_2}}{LG_2}\right\}$. For any $e_2(t) \in R/Q_1$, one has

$$|e_2| > \frac{\gamma_{\dot{D}_2}}{LG_2}.$$

This, together with (30) yields

$$\dot{V}_2 \leq -|e_2|(LG_2|e_2| - \gamma_{\dot{D}_2}) < 0.$$

Note that $G_2 = 1$. It implies that the steady error $e_2(t)$ will reach and stay in the following region

$$Q_1 = \left\{e_2 : |e_2| \leq \frac{\gamma_{\dot{D}_2}}{L}\right\}. \tag{31}$$

Now, we are ready to give the last result of the paper.

Theorem 2: If the composite TSM controller is designed as

$$\begin{aligned}\delta_f = \frac{1}{B_1}\Big(&-A_{11}r - A_{12}\hat{\beta} - c \cdot sign(r - r_d)|r - r_d|^{\alpha} - \hat{D}_2 \\ &-K_1 \cdot sign(s) - K_2 s\Big)\end{aligned} \tag{32}$$

where $k_1 > 0$, $k_2 > 0$ and $\hat{D}_2$ is generated by NDOB (28), then the yaw rate r will converge to its reference signal r_d in a finite time.

Proof: Substituting controller (32) into system (15) yields

$$\begin{aligned}\dot{s} &= -K_1 \cdot sign(s) - K_2 s + D_2(t) - \hat{D}_2 \\ &= -K_1 \cdot sign(s) - K_2 s + e_2(t). \end{aligned} \tag{33}$$

By the aforementioned NDOB (28), we know the error $e_2(t)$ is bounded. It implies that there exists a constant γ_{e_2} such that $|e_2(t)| = |D_2(t) - \hat{D}_2| \leq \gamma_{e_2}$. Then, it can be observed that system (33) has the same structure to system (17). The rest of proof is similar to that in Theorem 1. □

As a matter of fact, due to the fact that the estimation error $e_2(t)$ can be arbitrarily small, Theorem 2 reveals that the value of k_1 in controller (32) can be any positive constant, while the same gain in controller (16) should satisfy $k_1 > \gamma_{D_2}$. It can be concluded that the gain k_1 in the composite TSM controller has been significantly reduced. This also implies that the chattering can partially be attenuated.

Remark 3: For composite TSM controller (32), the parameters K_2 and α can be the same to that of controller (16), while the parameter K_1 can be chosen to be a rather smaller one. In addition, the parameter L in NDOB should be large in order to suppress the disturbance.

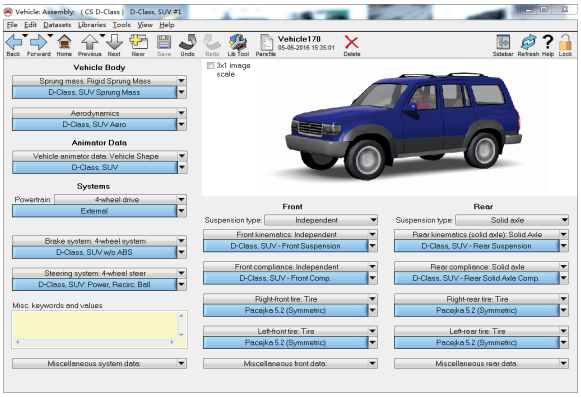

FIGURE 4. Carsim vehicle model.

IV. SIMULATION

In order to compare the effectiveness of four kinds of controllers, the vehicle model is established by a standard Carsim D-Class SUV. It should be noted that the tyre and chassis models are embedded in Carsim, therefore the longitudinal and lateral tire forces, yaw rate, sideslip angle, vehicle longitudinal and lateral velocity, etc, can be directly obtained by Carsim software. The command window of Carsim vehicle model of a four-wheel-drive vehicle is set as Fig. 4.

TABLE 1. Paraments of Vehicle Model.

Symbol	Description	Value
m	vehicle total mass	$1429(Kg)$
a	center of gravity to front axle distance	$1.05(m)$
b	center of gravity to rear axle distance	$1.569(m)$
I_z	yaw moment of inertia of vehicle	$1765(Kg \cdot m^2)$
C_f	equivalent nominal front-tire cornering stiffness	$79240(N/rad)$
C_r	equivalent nominal rear-tire cornering stiffness	$87002(N/rad)$
n	gear ratio	20

The key parameters of the vehicle model in simulation are presented in Table 1.

TABLE 2. Paraments of Controllers.

Controllers	Paramenters
PI (13)	$K_p = 35, K_i = 5$
TSM (16)	$K_1 = 8000, K_2 = 760, c = 1, \alpha = 1/3$
PI+DOB (26)	$K_p = 35, K_i = 5, Q(s) = \frac{1}{0.01s+1}$
TSM+NDOB (32)	$K_1 = 330, K_2 = 760, c = 1, \alpha = 1/3, L = 6000$

The initial speed of vehicle is taken as $80km/h$, the maximum steering wheel angle is $60deg$, and the road adhesion coefficient μ is chosen as 0.3. Additionally, the parameters of all the four controllers (13), (16), (26), and (32) are shown in Table 2.

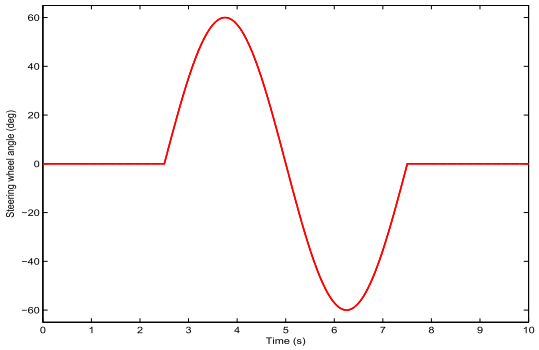

FIGURE 5. Steering wheel angle.

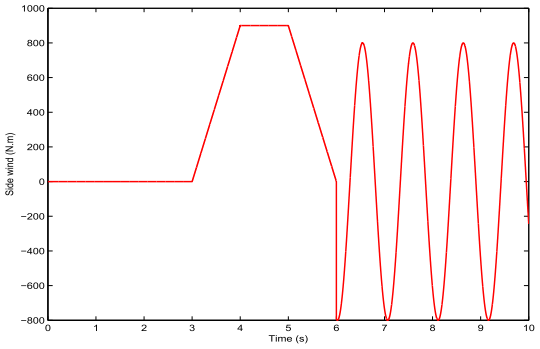

FIGURE 8. The side wind disturbance input.

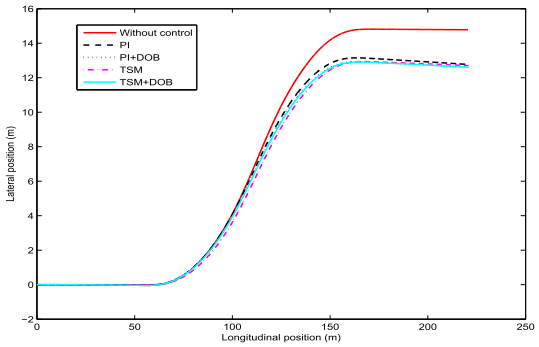

FIGURE 6. The vehicle trajectory under different controllers in the case of single lane change maneuver (without side wind disturbance).

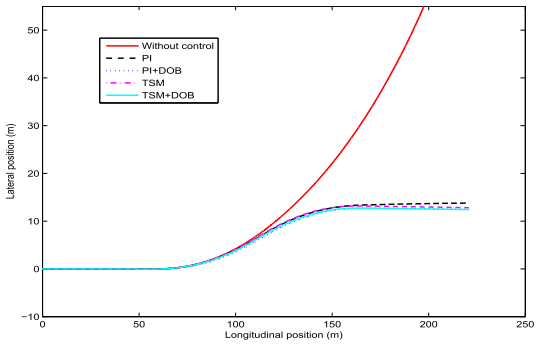

FIGURE 9. The vehicle trajectory under different controllers in the case of single lane change maneuver (with side wind disturbance).

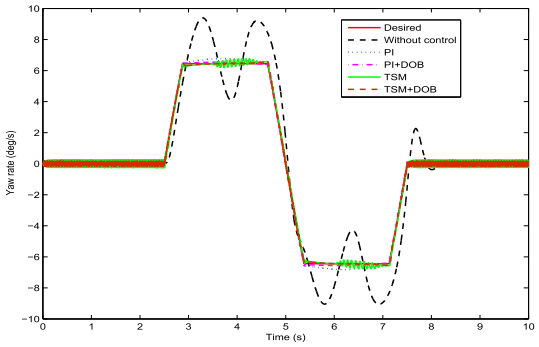

FIGURE 7. The response curves of yaw rate under different controllers in the case of single lane change maneuver (without side wind disturbance).

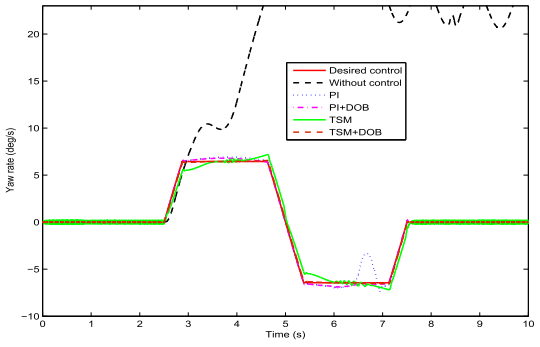

FIGURE 10. The response curve of yaw rate under different controllers in the case of single lane change maneuver (with side wind disturbance).

A. SINGLE LANE CHANGE MANEUVER WITHOUT SIDE WIND DISTURBANCE

For the case of single lane change, the steering wheel angle is regarded as the input of the system, which is shown in Fig. 5. Without considering the effect of side wind disturbance, the simulation results are shown in Figs. 6-7, where Fig. 6 gives the vehicle trajectories and Fig. 7 shows the time history of yaw rate. From Fig. 7, it can be clearly seen that without control the yaw rate is unstable, while it can well track the reference signal under the given four kinds of controllers. Consequently, we could arrive at a conclusion that all the four kinds of controllers have positive impacts on AFS system.

B. SINGLE LANE CHANGE MANEUVER UNDER SIDE WIND DISTURBANCE

To compare the robustness of the proposed controllers, the effect of side wind disturbance has been taken into account. The simulation is conducted under a side wind force, which is shown in Fig. 8. By Fig. 8, we can observe that the side wind disturbance includes step, ramp and sinusoidal signals. It can be seen from Fig. 9 and Fig. 10 that, the PI controller fails to keep the stability, while the other three controllers can well keep vehicle's stability. As a matter of fact, by Fig. 10, it can also be concluded that the PI controller can overcome the influences of the step and ramp signals, but can not well handle the sinusoidal disturbance. However, the PI controller still

works if the DOB can be used to compensate the disturbance. In addition, we can also see that the control performance under composite controller is better than that under the pure state-feedback controller.

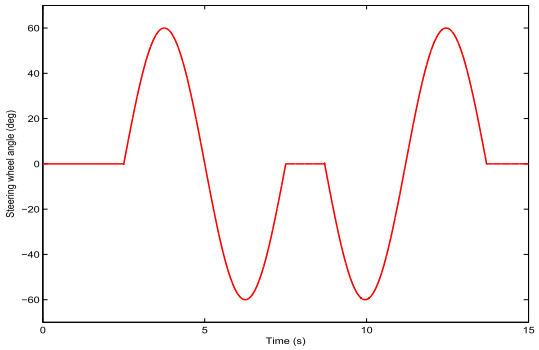

FIGURE 11. Steering wheel angle.

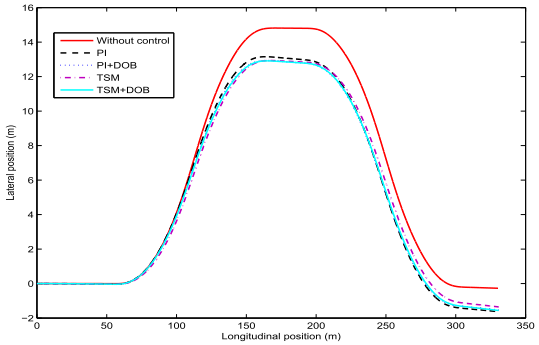

FIGURE 12. The vehicle trajectory under different controllers in the case of double lane change maneuver (without side wind disturbance).

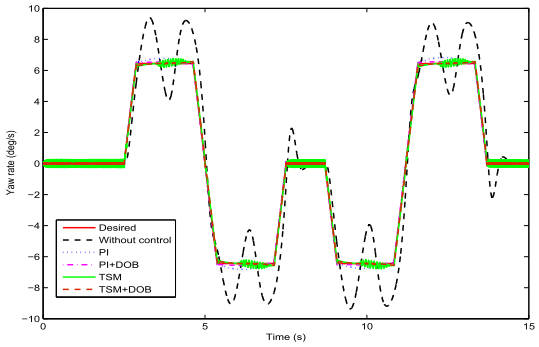

FIGURE 13. The response curves of yaw rate under different controllers in the case of double lane change maneuver (without side wind disturbance).

C. DOUBLE LANE CHANGE MANEUVER WITHOUT SIDE WIND DISTURBANCE

Consider the double lane change maneuver, as is shown in Fig. 11. Under the baseline controllers (13), (16) and the composite controllers (26), (32), without considering the effect of side wind disturbance, simulation results are shown in Figs. 12-13. Specifically, Fig. 12 depicts the vehicle trajectory and Fig. 13 gives the time history of the yaw rate. It can be clearly seen that without control the yaw rate is unstable, while the four kinds of controllers designed in this paper are all effective in keeping the stability of the vehicle. Also, we can observe from Fig. 13 that the tracking performance under composite controllers are better than that under baseline controllers.

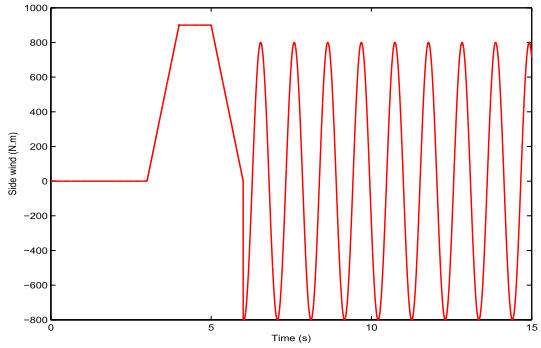

FIGURE 14. The side wind disturbance input.

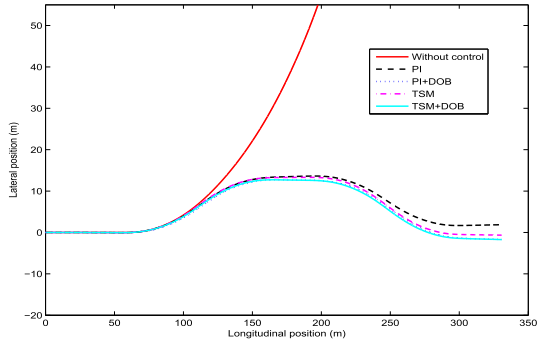

FIGURE 15. The vehicle trajectory under different controllers in the case of double lane change maneuver (with side wind disturbance).

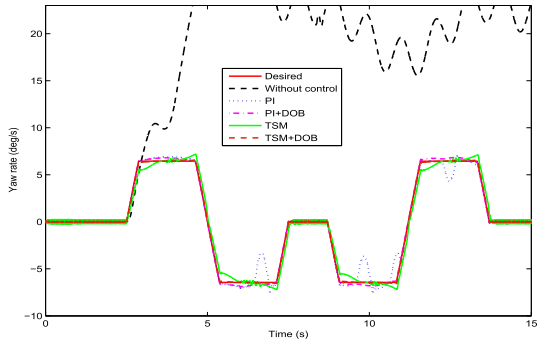

FIGURE 16. The response curves of yaw rate under different controllers in the case of double lane change maneuver (with side wind disturbance).

D. DOUBLE LANE CHANGE MANEUVER WITH SIDE WIND DISTURBANCE

Finally, side wind disturbance is also considered for double lane change maneuver so as to compare the robustness between the baseline controllers (13), (16) and the composite controllers (26), (32). Fig. 14 displays the time history of the side wind. Fig. 15 plots the vehicle trajectory. Fig. 16 gives the response curves of the yaw rate. By Fig. 15 and Fig. 16, it can be observed that the PI controller fails to keep the stability

and the performance under TSM controller is also not satisfactory. This implies that the pure state-feedback control used to suppress the large disturbance may also bring some adverse effects. To fix this problem, the composite control is one of effective solutions. Under the composite control schemes, the side wind disturbance can first be estimated by NDOB and then be compensated. This property can be reflected in Fig. 16, where the composite controllers (26), (32) exhibit better performance than the baseline controllers (13), (16).

V. CONCLUSIONS

In this paper, four kinds of AFS controllers are proposed for keeping the stability of a vehicle. The first two baseline controllers are respectively constructed based on PI control and terminal sliding mode control technique, such that the yaw rate will track its desired value. However, under some large disturbances, the performance under the baseline controllers are not satisfactory. To further improve the robustness of the AFS system, the composite AFS controllers are also developed by combining the baseline controllers and the disturbance observer technique. The validity of the proposed AFS controllers are verified by using Carsim software. From simulation results, it can easily make a conclusion that the composite TSM controller possesses the best control performance. It should also be pointed out that the active safety control under pure AFS are not enough under some cases. A more effective method is the AFS and DYC integrated control. Our future work will focus on the active safety control by combining the direct yaw moment control and AFS.

REFERENCES

[1] S. Perić, D. Antić, M. Milovanović, D. Mitić, M. Milojković, and S. Nikolić, "Quasi-sliding mode control with orthogonal endocrine neural network-based estimator applied in anti-lock braking system," *IEEE-ASME Trans. Mechatron.*, vol. 21, no. 2, pp. 754–764, Feb. 2016.

[2] Y. Shibahata, K. Shimada, and T. Tomari, "Improvement of vehicle maneuverability by direct yaw moment control," *Veh. Syst. Dyn.*, vol. 22, nos. 5–6, pp. 465–481, 1993.

[3] W. Sun, H. Gao, and B. Yao, "Adaptive robust vibration control of full-car active suspensions with electrohydraulic actuators," *IEEE Trans. Control Syst. Technol.*, vol. 21, no. 6, pp. 2417–2422, Jun. 2013.

[4] W. Sun, H. Pan, and H. Gao, "Filter-based adaptive vibration control for active vehicle suspensions with electrohydraulic actuators," *IEEE Trans. Veh. Technol.*, vol. 65, no. 6, pp. 4619–4626, Jun. 2016.

[5] S. Di Cairano, H. E. Tseng, D. Bernardini, and A. Bemporad, "Vehicle yaw stability control by coordinated active front steering and differential braking in the tire sideslip angles domain," *IEEE Trans. Control Syst. Technol.*, vol. 21, no. 4, pp. 1236–1248, Apr. 2013.

[6] J. Ackermann, "Robust control prevents car skidding," *IEEE Control Syst.*, vol. 17, no. 3, pp. 23–31, Mar. 1997.

[7] S. Mammar and D. Koenig, "Vehicle handling improvement by active steering," *Veh. Syst. Dyn.*, vol. 38, no. 38, pp. 211–242, 2002.

[8] P. Falconea, H. Tsengb, F. Borrellic, J. Asgarib, and D. Hrovatb, "MPC-based yaw and lateral stabilisation via active front steering and braking," *Veh. Syst. Dyn.*, vol. 46, no. S1, pp. 611–628, 2008.

[9] Q. Li, G. Shi, J. Wei, and Y. Lin, "Yaw stability control of active front steering with fractional-order PID controller," in *Proc. Int. Conf. Inf. Eng. Comput. Sci.*, 2009, pp. 1–4.

[10] Z. Chen, B. Yao, and Q. Wang, "μ-Synthesis-based adaptive robust control of linear motor driven stages with high-frequency dynamics: A case study," *IEEE/ASME Trans. Mechatron.*, vol. 20, no. 3, pp. 1482–1490, Mar. 2015.

[11] Z. Chen, Y. Pan, and J. Gu, "Integrated adaptive robust control for multilateral teleoperation systems under arbitrary time delays," *Int. J. Robust Nonlinear Control*, vol. 26, no. 12, pp. 2708–2728, 2016.

[12] Z. Chen, Y.-J. Pan, and J. Gu, "A novel adaptive robust control architecture for bilateral teleoperation systems under time-varying delays," *Int. J. Robust Nonlinear Control*, vol. 25, no. 17, pp. 3349–3366, 2015.

[13] C. March and T. Shim, "Integrated control of suspension and front steering to enhance vehicle handling," *Proc. Inst. Mech. Eng. D J. Autom. Eng.*, vol. 221, no. 221, pp. 377–391, 2007.

[14] M. Nagai and M. Shino, "Study on integrated control of active front steer angle and direct yaw moment," *JSAE Rev.*, vol. 23, no. 3, pp. 309–315, 2002.

[15] J. Park and W. Ahn, "H_∞ yaw-moment control with brakes for improving driving performance and stability," in *Proc. Int. Conf. Adv. Intell. Mechatron.*, 1999, pp. 747–752.

[16] M. Akar and J. C. Kalkkuhl, "Lateral dynamics emulation via a four-wheel steering vehicle," *Vehicle Syst. Dyn., Int. J. Vehicle Mech. Mobility*, vol. 46, no. 9, pp. 803–829, 2008.

[17] Q. Zhou, F. Wang, and L. Li, "Robust sliding mode control of 4WS vehicles for automatic path tracking," in *Proc. IEEE Intell. Veh. Symp.*, Sep. 2005, pp. 819–826.

[18] S. H. Ding, L. Liu, and W. Zheng, "Sliding mode direct yaw-moment control design for in-wheel electric vehicles," *IEEE Trans. Ind. Electron.* doi: 10.1109/TIE.2017.2682024.

[19] S. H. Ding and J. L. Sun, "Direct yaw-moment control for 4WID electric vehicle via finite-time control technique," *Nonlinear Dyn.*, vol. 88, no. 1, pp. 239–254, 2017.

[20] M. Zhihong, A. P. Paplinski, and H. R. Wu, "A robust MIMO terminal sliding mode control scheme for rigid robotic manipulators," *IEEE Trans. Autom. Control*, vol. 39, no. 12, pp. 2464–2469, Dec. 1994.

[21] S. Yu, X. Yu, B. Shirinzadeh, and Z. Man, "Continuous finite-time control for robotic manipulators with terminal sliding mode," *Automatica*, vol. 41, no. 11, pp. 1957–1964, Nov. 2005.

[22] Q. Zhou, D. Yao, J. Wang, and C. Wu, "Robust control of uncertain semi-Markovian jump systems using sliding mode control method," *Appl. Math. Comput.*, vol. 286, pp. 72–87, Sep. 2016.

[23] Y. Feng, J. Zheng, X. Yu, and N. V. Truong, "Hybrid terminal sliding-mode observer design method for a permanent-magnet synchronous motor control system," *IEEE Trans. Ind. Electron.*, vol. 56, no. 9, pp. 3424–3431, Sep. 2009.

[24] S. H. Ding and S. H. Li, "Second-order sliding mode controller design subject to mismatched term," *Automatica*, vol. 77, pp. 388–392, Mar. 2017.

[25] W.-H. Chen, "Nonlinear disturbance observer-enhanced dynamic inversion control of missiles," *J. Guid., Control, Dyn.*, vol. 26, no. 1, pp. 161–166, Jan. 2003.

[26] Y. Ji, H. Guo, and H. Chen, "Integrated control of active front steering and direct yaw moment based on model predictive control," in *Proc. 26th Chin. Control Decision Conf.*, 2014, pp. 2044–2049.

[27] N. Yu, *Yaw-Control Enhancement for Buses by Active Front-Wheel Steering*. Pennsylvania, PA, USA: Pennsylvania State Univ., 2007.

[28] R. Rajamani, *Vehicle Dynamics and Control*. New York, NY, USA: Springer-Verlag, 2011, ch. 8.

[29] Y. Shtessel, C. Edwards, L. Fridman, A. Levant, *Sliding Mode Control and Observation*. New York, NY, USA: Springer, 2014.

[30] S. H. Ding, A. Levant, and S. H. Li, "Simple homogeneous sliding-mode controller," *Automatica*, vol. 67, pp. 22–32, Sep. 2016.

[31] S. Li, J. Yang, W. Chen, X. Chen, *Disturbance Observer-Based Control: Methods and Applications*. Boca Raton, FL, USA: CRC Press, 2014.

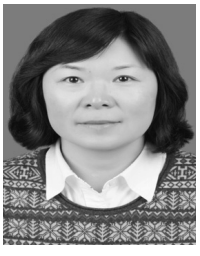

XIAOYAN DIAO was born in Jiangsu, China, in 1978. She received the B.E. and M.S. degrees in electrical engineering from Jiangsu University, China, in 2001 and 2008, respectively. She is currently an Assistant Professor with the School of Electrical and Information Engineering, Jiangsu University. Her current research interests include PMSM, sliding mode control, and vehicle safety control.

YANG JIN was born in Jiangsu, China, in 1992. She is currently pursuing the master's degree with the School of Electrical and Information Engineering, Jiangsu University. Her main research interests are vehicle dynamics and nonlinear control theory.

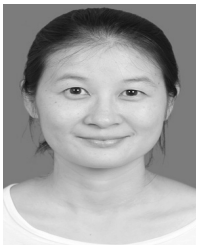

LI MA was born in Anhui, China, in 1982. She received the B.S. and M.S. degrees in mathematics from Anhui Normal University, Wuhu, China, in 2004 and 2007, respectively, and the Ph.D. degree from the School of Automation, Southeast University, Nanjing, China, in 2011. She is currently an Associate Professor with the School of Electrical and Information Engineering, Jiangsu University, Zhenjiang, China. Her current research interests include vehicle dynamics and sliding mode control theory.

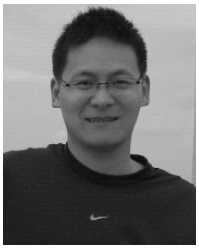

SHIHONG DING was born in Anhui, China, in 1983. He received the B.E. degree in mathematics from Anhui Normal University, China, in 2004, and the M.S. degree and the Ph.D. degree in automatic control from Southeast University, China, in 2007 and 2010, respectively. During his graduate studies, he visited The University of Texas at San Antonio from 2008 to 2009. Since graduation, he has held a Research Fellowship with the University of Western Sydney. He is currently an Associate Professor with the School of Electrical and Information Engineering, Jiangsu University. His current research interests include sliding mode control and finite-time stability.

HAOBIN JIANG was born in Jiangsu, China, in 1969. He received the B.E. degree in agricultural machinery from Nanjing Agricultural University, China, in 1991, and the M.S. degree and the Ph.D. degree in automotive engineering from Jiangsu University, China, in 1994 and 2000, respectively. He is currently a Professor with the School of Automotive and Traffic Engineering, Jiangsu University. His current research interests include vehicle dynamics.